Noncontact measurement of liquid-surface properties with knife-edge electric field tweezers technique

Yuji Shimokawa and Keiji Sakai
Institute of Industrial Science, The University of Tokyo, 4-6-1 Komaba, Meguro-ku, Tokyo 153-8505, Japan
(Received 4 February 2013; published 17 June 2013)

We have developed a technique for the simultaneous measurement of the surface tension and the viscosity of a liquid in a noncontact manner. In this method, a small linear deformation of the liquid surface is induced by a local dielectric force that is brought about by a knife-edge electrode. The surface tension and the viscosity are obtained from the shape of the induced meniscus and from the dynamic response of the surface, respectively. The surface tension obtained was examined in comparison with the values measured by the Wilhelmy plate method. We also measured time constants of the surface deformation for a variety of standard viscosity samples and obtained the relation between the time constant and the viscosity. The demonstrated advantage of the system is the ability to uniquely determine the surface tension and the viscosity.

DOI: 10.1103/PhysRevE.87.063009 PACS number(s): 47.61.−k, 47.80.−v

I. INTRODUCTION

Surface properties such as the surface tension and surface viscoelasticity are of great importance in the field of microfluidics. Fluid systems such as microchannels [1], inkjet systems [2–6], and precision coatings [7–10] are becoming progressively smaller in size. In such small systems, whose characteristic length is shorter than the capillary length, the contribution of the surface becomes significant. Consequently, in these systems, the surface tension plays an important role in determining the fluid dynamics.

Some widely used methods for the measurement of the surface tension include the Wilhelmy plate method [11], the pendant drop method [12], and the capillary rise method. These methods require a solid probe or a solid wall to be in contact with the sample liquid surface; yet, contact of a probe with the liquid surface is often problematic. For instance, the surface of the liquid or the equipment might become contaminated. Instabilities caused by complex interactions between the solid surface and substances dissolved in solutions are also troublesome.

Recently, we developed an electric field tweezers system to measure surface properties without contacting the liquid surface [13]. In the electric field tweezers method, the sample surface is deformed by the electric field that is formed near the tip of a needle electrode, and the sample viscosity is obtained from the time constant of the dynamic response of the surface [14–16]. Because the electric field is localized in a small surface area ($\sim$100 μm^2), the time constant, which is proportional to the localization length, is small. Consequently, rapid measurements can be carried out even for highly viscous samples. However, by using the previous method, we cannot uniquely determine both the surface tension and the viscosity, because the time constant is given by their ratio. In our previous work, the known surface tension of pure water was used as a reference, and the measured surface tension of a surfactant solution was compared against this reference.

In this paper, we report a different method, using which an absolute value of the surface tension can be obtained by measuring the shape of a deformed surface. In this method, a metal blade instead of a needle is used as the electrode, and a small deformation of the liquid surface is detected by an optical lever technique with multiple laser beams. In addition, we demonstrate that the time constant of the surface deformation can also be measured with the same setup, yielding the value of the sample's viscosity.

II. EXPERIMENT

A. Principle and experimental setup

Figure 1(a) shows a schematic diagram of our system. A Petri dish containing a liquid sample is placed on a metal plate that is connected to the ground. The diameter of the Petri dish is 85 mm, and the thickness of the liquid samples is 2–3 mm. A 35-mm-long metal blade electrode is placed 250 μm above the sample surface, with its edge parallel to the sample surface. The electric signal from a function generator (WF1956, NF Co., Japan) is amplified by a high-voltage amplifier (HOPS-3P1, Matsusada Precision Inc., Japan) and is provided to the blade electrode.

A thin linear electric field, formed around the knife edge of the blade electrode, applies a dielectric force and picks up the liquid surface, inducing a small deformation. In the experiment, a high-frequency alternating electric field, whose frequency is 1 kHz, was applied instead of a dc field to avoid the electrical charging up of the sample surface. Since the carrier frequency is sufficiently higher than the characteristic frequency of the surface response, the electric field can be regarded as a modulated dc signal. We consider the orthogonal coordinates shown in Fig. 1(b), in which the x and y axes in the horizontal plane are perpendicular and parallel to the edge of the blade electrode, respectively. Since the electric field and the deformation of the liquid surface have translational symmetry along the y axis, it is possible to consider the shape of the surface deformation only in the xz plane. Let $\zeta(x)$ be the vertical displacement at the coordinate x. When the state of equilibrium is achieved, $\zeta(x)$ is determined from the balance of the Laplace pressure, the gravity, and the dielectric force, and $\zeta(x)$ satisfies the following force balance equation:

$$-\gamma\frac{d^2\zeta}{dx^2}+\rho g\zeta = P(x), \tag{1}$$

where γ, ρ, and g are the surface tension, the density, and the acceleration due to gravity, respectively. The term

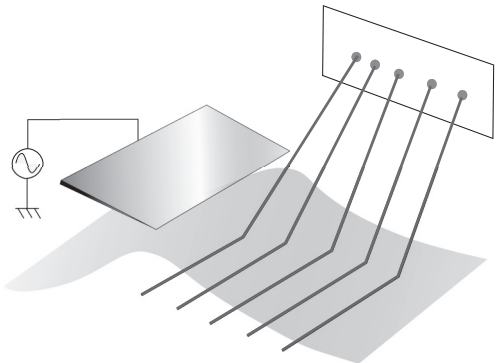

(a)

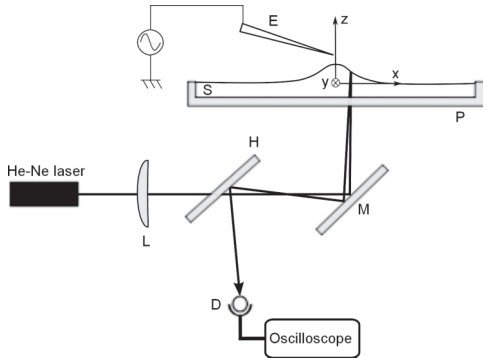

(b)

FIG. 1. (a) Schematic illustration of the knife-edge electric field tweezers method. The surface deformation, induced by the dielectric force, is measured by laser beams aligned in parallel, and the surface tension is obtained from the shape of a meniscus. (b) Schematic illustration of the viscosity measurement. L, lens ($f = 200$ mm); H, half mirror; M, mirror; P, Petri dish; S, liquid sample; E, blade electrode; D, position-sensitive detector.

$P(x)$ represents the spatial distribution of the dielectric force.

When high voltage is applied to the knife-edge electrode, almost all of the charge is localized at the edge, and it can be approximately regarded as a line charge. However, a slight charge that remains in the blade plane influences the dielectric force on the surface. The blade is therefore tilted by 60° from the perpendicular, whereby half of the surface area $x > 0$, is not affected by the charge that is not localized at the knife edge.

For a linear charge distributed along the length ℓ with charge density λ, the explicit expression for $P(x)$ can be obtained using the method of image charges:

$$P(x) = \frac{\lambda^2 \ell^2}{8\pi^2 \varepsilon_0} \frac{\varepsilon_r - 1}{(\varepsilon_r + 1)^2} \frac{1}{(x^2 + h^2)^2} \frac{x^2 + \varepsilon_r h^2}{x^2 + h^2 + (\ell/2)^2}, \quad (2)$$

where ε_0 is the permittivity of vacuum, ε_r is the relative permittivity of the sample, h is the gap between the knife edge and the horizontal surface, and ℓ is the length of the knife edge [17]. Since a strong electric field is localized near the sharp edge, the dielectric force acting on the liquid surface is localized approximately within the length of the gap between the edge of the electrode and the sample surface. The dielectric force $P(x)$ is negligible if $h \ll x$, and the right-hand side of Eq. (1) can be set to zero. Thus, the solution can be approximated to

$$\zeta(x) = A \exp(-\kappa x), \quad (3)$$

where A is a constant, and κ is the inverse of the capillary length:

$$\kappa = \sqrt{\frac{\rho g}{\gamma}}. \quad (4)$$

This solution represents the so-called meniscus, and the surface tension γ can be obtained from Eq. (4), provided the density ρ and the experimental value of κ are known.

B. Measurement of surface tension

To obtain the surface tension from the shape of a meniscus, we should observe a slightly deformed shape of the sample surface over a large surface area. To this end, we used an optical lever technique that allows the detection of the small deformation of the liquid surface that is induced by the dielectric force. A laser beam, emitted from a frequency-doubled Nd:YAG laser (10 mW), is expanded and collimated by an optical lens system and is focused by a cylindrical lens to form a laser sheet. Then, the laser sheet passes through a transparent film with a grid pattern printed in black (spacing and linewidth are both 0.3 mm), forming multiple laser beams aligned in parallel. As shown in Fig. 1(a), the laser beams are reflected at the sample surface and projected on the screen placed above the sample. The position of each bright point on the screen is then captured using a charge coupled device (CCD) camera. The bright points are regularly distributed when the surface is flat, but their positions change when the surface is curved. The gradient of the surface $d\zeta/dx$ is approximately given by

$$\frac{d\zeta}{dx} = -\frac{\Delta X}{2L}, \quad (5)$$

where ΔX is the displacement of the bright points and L is the vertical distance from the surface to the bright points. To effectively increase the number of measuring points and improve the spatial resolution of the measurement, the grid is shifted five times (in steps of 100 μm) by an automatic positioning stage.

Figure 2 shows examples of the surface tension measurement for propylene glycol and toluene; these experiments were conducted at 30 °C. Although the data obtained from the optical lever technique are the spatial derivatives $d\zeta/dx$, rather than the actual surface shape $\zeta(x)$, we did not integrate the data to obtain the actual shape of the meniscus, because the exponential function remains unchanged for the differential operations. The solid line in Fig. 2(a) shows an exponential function fitted to the experimental data in the range of $1.5 < x < 10$ mm, preventing the effect of the localized dielectric force near the electrode. From the fitted curve in Fig. 2(a), we obtained $\kappa = 0.509$ mm^{-1}. With a density of $\rho = 1.018$ g/cm^3, as measured by a graduated cylinder and an electronic balance (TE1520S, Sartorius Mechatronics Japan K.K., Japan), the surface tension was determined to be $\gamma = 38.5$ mN/m. The value obtained using the Wilhelmy plate

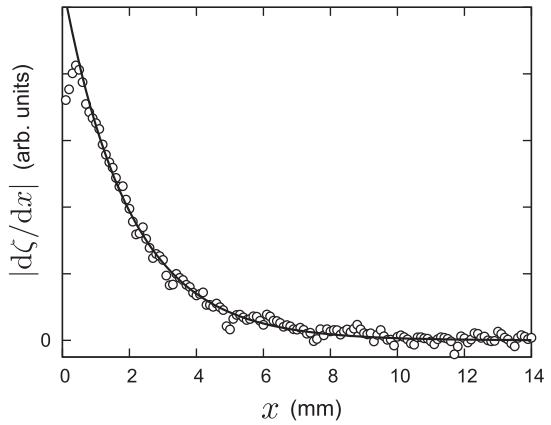

(a)

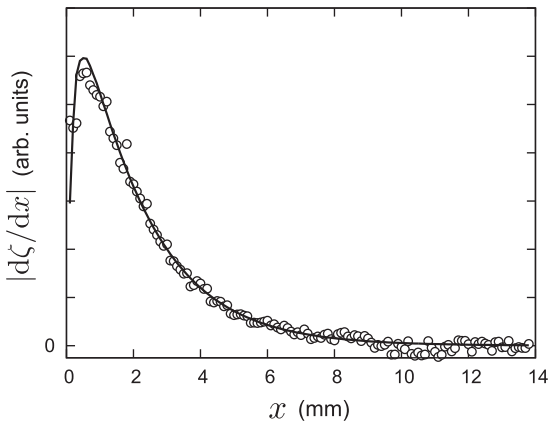

(b)

FIG. 2. The derivative of the deformed surface for propylene glycol (a) and for toluene (b). The solid line shows the fitting curve of the exponential function (a) and of the exact solution of Eq. (1), including the effect of the dielectric force (b).

method was $\gamma = 35.8$ mN/m, and the deviation between the values was about 7%.

On the other hand, measuring the surface tension of low-permittivity samples such as nonpolar liquids requires a stricter approach. This is attributed to the fact that the dielectric force extends to a long distance from the electrode, and the shape of the meniscus can no longer be approximated by a simple exponential function. Therefore, we need to take into account the distribution of the dielectric force. By solving Eqs. (1) and (2), we obtain the strict solution for the deformed surface [17]. Figure 2(b) shows the result obtained for toluene, with $\varepsilon_r = 2.3$, used as a low-permittivity sample. The solid line in Fig. 2(b) shows the strict solution fitted to the experimental data. From the fitting results, we obtain $\kappa = 0.535$ mm^{-1} as the fitting parameter. With the density $\rho = 0.848$ g/cm^3, the surface tension is calculated to be $\gamma = 29.0$ mN/m. The surface tension measured by the Wilhelmy plate method is $\gamma = 27.4$ mN/m, and the deviation between the two values is about 6%. This analysis requires the permittivity of the measured sample to be known in advance.

Figure 3 shows a comparison between the surface tension obtained using the present method, and the one obtained using

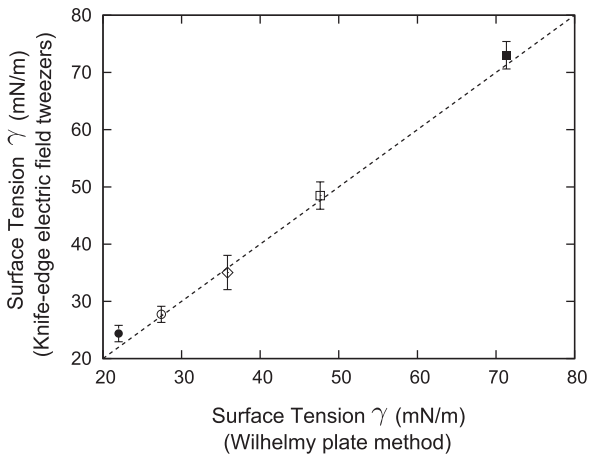

FIG. 3. The comparison between the surface tension values measured by the knife-edge electric field tweezers method and by the Wilhelmy plate method. •, ethanol; ○, toluene; ◇, propylene glycol; □, ethylene glycol; ■, distilled water. The experiment was conducted at 30 °C. Each sample was measured three times and the standard deviation is shown as the error bars. Note that only the value for toluene was determined by fitting with the exact solution of Eq. (1). The dashed line (slope of unity) corresponds to a complete agreement between the surface tension values measured with the two methods.

the Wilhelmy plate method [18]. Disagreement between the results of these two methods, seen in Fig. 3, would be mainly due to the mechanical noise that represents a vibration of the liquid. Accuracy of the measurement would be improved by employing a mechanical noise damper.

C. Measurement of viscosity

In our knife-edge electric field tweezers method, the viscosity of liquid samples can be obtained from the dynamic response of the sample surface. When the electric field is turned on and off, the sample surface shows a transient behavior and finally reaches an equilibrium state. In the area $x < \kappa^{-1}$, the effect of gravity is negligible and the dynamic behavior of the surface is determined only by the viscosity and surface tension.

Figure 1(b) shows a schematic diagram of the experimental configuration that was used to measure the viscosity. In this configuration, a laser beam from a He-Ne laser was focused by a lens ($f = 200$ mm), and made incident on the sample from the underside of a Petri dish. This incident laser beam was reflected from the sample surface, and it traveled backward, almost collinear with the incident beam. Following this, the laser beam was reflected by a half mirror, and the deflection was detected by a position-sensitive detector (PSD; S1352, Hamamatsu Photonics K.K., Japan). The deformation curve of the sample surface exhibited an exponential decay, following the rectangular modulation of the electric field [13,17,19]. In our experiments, we obtained a time constant τ of the surface deformation by fitting an exponential function to the transient signal that was obtained after the electric field was turned off.

Figure 4 shows the time constants obtained for a series of silicone oils whose viscosity values ranged from 0.0017 to 978 Pa s. It is seen that the time constants obtained for highly viscous samples are proportional to their corresponding

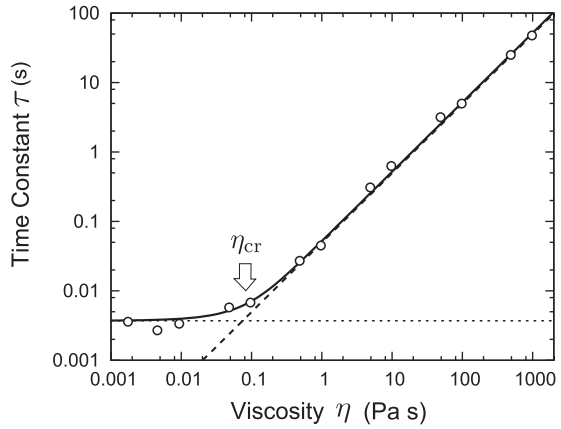

FIG. 4. The relation between the time constant of the step response τ and the viscosity η. The samples are a series of standard silicone oils whose viscosities are known. The experiment was conducted at 35 °C. The peak-to-peak amplitude of the applied voltage was 900 V, and the frequency was 1 kHz. The time constant was obtained after the electric field was turned off. The effect of inertia appeared near the characteristic viscosity $\eta_{cr} = \sqrt{\rho\gamma h} \sim 0.07$ Pa s, making the relation deviate from linearity.

viscosities, whereas those for low-viscosity samples are not linearly related to their viscosities. To discuss the relation between τ and η, we used the Stokes equation in the lubrication approximation. In our method, the area in which the dielectric force acts on the liquid surface is limited by the same spatial scale as the gap h between the knife edge and the liquid surface. Therefore, a projection that is induced by the electric field below the electrode is localized within the length h. The penetration depth of the surface motion is also limited by h. Therefore, for the region deeper than h, we neglected the detailed distribution of the velocity field in the sample fluid (refer to Fig. 5 in the Appendix).

To discuss the surface behavior of highly viscous liquids, we start with the Stokes equation:

$$\eta \frac{\partial^2 v}{\partial z^2} = \frac{\partial p_L}{\partial x}. \tag{6}$$

In Eq. (6), $v = v(t,x,z)$ is the horizontal component of the velocity field and p_L is the Laplace pressure. It should be noted that the effect of gravity is negligible, because the spatial scale of the relevant surface deformation is much smaller than the capillary length. Let us suppose that the velocity field is the Poiseuille flow driven by the Laplace pressure and that it satisfies the following boundary conditions:

$$v(t,x,z=-h) = 0, \qquad \left.\frac{\partial v}{\partial z}\right|_{z=0} = 0. \tag{7}$$

Here, we estimate the magnitude of each term in Eq. (6). The average velocity of the velocity field and the Laplace pressure are estimated as $v \sim \zeta_0/\tau$ and $p_L \sim \gamma\zeta_0/h^2$, respectively, where $\zeta_0 = \zeta(x=0)$. Since the characteristic length of the system is only h, we obtain the following estimations:

$$\eta \frac{\partial^2 v}{\partial z^2} \sim -\frac{\eta\zeta_0}{h^2\tau}, \tag{8}$$

$$\frac{\partial p_L}{\partial x} \sim -\gamma\frac{\zeta_0}{h^3}. \tag{9}$$

Substituting these estimations into Eq. (6), we obtain the following linear relation:

$$\tau = \frac{\alpha\eta h}{\gamma}, \tag{10}$$

where α is a constant. In the analysis of experimental results, α is treated as a fitting parameter. The dashed line in Fig. 4 shows the best fit to the linear relation in Eq. (10). Setting $h = 250$ μm and $\gamma = 21.3$ mN/m [20], the coefficient is determined as $\alpha = 4.19$. The absolute values of the sample viscosity can be obtained from Eq. (10) using the value of α (as above) and the experimentally obtained value of the surface tension.

In contrast, in the low-viscosity regime, the time constant τ is not linearly related to the viscosity. In this regime, the effect of inertia becomes apparent and the approximated Stokes equation [Eq. (6)] no longer holds. Further, in this low-viscosity limit, the dispersion relation of the surface-capillary wave is [19]

$$\tau \sim \sqrt{\frac{\rho}{\gamma}} h^{3/2}. \tag{11}$$

The dispersion relation is shown as a dotted line in Fig. 4. Here, we estimate the lower limit of the viscosity η_{cr} that can be measured using the present method; this gives the crossover from the viscous case described by Eq. (10) to the inertia scenario given by Eq. (11). By using Eqs. (10) and (11), we obtain

$$\eta_{cr} \equiv \sqrt{\rho\gamma h}. \tag{12}$$

In Fig. 4, the characteristic viscosity of $\eta_{cr} = 0.07$ Pa s is indicated by an arrow. When the viscosity is close to η_{cr}, the following equation gives a first-order approximation for τ:

$$\tau = \frac{\alpha\eta h}{2\gamma}\left(1 + \sqrt{1 + \frac{4\eta_{cr}^2}{\eta^2}}\right). \tag{13}$$

The derivation of Eq. (13) is given in the Appendix. The relation between τ and h, calculated using Eq. (13), is shown as a solid line in Fig. 4, and it can be seen that the curve is in good agreement with the experimental data. This result shows that the viscosity can be accurately obtained from the time constant of the surface deformation, although the effect of inertia is not negligible. As can be seen from Eq. (13), in the low-viscosity regime ($\eta < \eta_{cr}$), the time constant is almost independent of the viscosity and the error in determining the viscosity rapidly increases. Actually, in the other conventional methods, accurate determination of a low viscosity is also found to be difficult. Recently, a method which is suitable for the measurement of low viscosity has been proposed by Hosoda *et al.*, and the method can supplement the experimental data in the low-viscosity regime [21].

III. CONCLUSIONS

We developed a knife-edge electric field tweezers method to simultaneously measure the surface tension and the viscosity of liquid samples, without the need to contact the sample surface. The surface tension and the viscosity are determined from the shape of a meniscus and the time constant of a step

response, respectively. With the previous method that used electric field tweezers, only the ratio γ/η was obtained [13], whereas the present method allows unique determination of the absolute values of the parameters γ and η. The main advantage of this technique is that it prevents the various types of damage caused by the contact of a probe with the sample surface.

This technique is useful for investigations of the delicate surface properties of liquid samples. We are trying to extend the method to measure more complex fluids such as viscoelastic fluids, and the result will be reported soon.

ACKNOWLEDGMENTS

The authors would like to thank S. Mitani, T. Hirano, T. Nagashima, and Y. Matsuura (IIS, The University of Tokyo) for useful discussions and their help in the experiment.

APPENDIX

In the high-viscosity regime, $\eta_{cr} \ll \eta$, the time constant τ of the surface deformation is proportional to the viscosity η (Fig. 4). On the other hand, in the intermediate-viscosity regime, $\eta \sim \eta_{cr}$, the linear relation [as in Eq. (10)] needs to be modified to account for the effect of inertia. Here, we take the effect of inertia into account and derive the relation between τ and η for the intermediate-viscosity regime. We start with the Navier-Stokes equation

$$\rho\frac{\partial v}{\partial t} = -\frac{\partial p_L}{\partial x} + \eta\frac{\partial^2 v}{\partial z^2}, \tag{A1}$$

where $v = v(t,x,z)$ is the horizontal component of the velocity field and p_L is the Laplace pressure. The left-hand side of Eq. (A1) shows the effect of inertia, and this effect is not negligible when the Reynolds number $\mathrm{Re} \sim (\eta_{cr}/\eta)^2$ approaches the value of unity. Note that the nonlinear term in the Navier-Stokes equation can be neglected in our system, because the velocity gradient with respect to the horizontal direction is small.

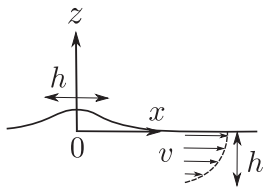

FIG. 5. The profile of the velocity field, after the electric field is turned off. In the region deeper than h, the liquid is static all the time. Since the liquid flow is driven by the Laplace pressure, the profile of the velocity field is approximately parabolic (Poiseuille flow).

Figure 5 shows a schematic diagram of the velocity field after the electric field is turned off. We estimate each term in Eq. (A1) with the characteristic length h and the time constant τ. These two terms on the right-hand side of Eq. (A1) are estimated using Eqs. (8) and (9). The left-hand side is estimated as

$$\rho\frac{\partial v}{\partial t} \sim \frac{\rho\zeta_0}{\tau^2}, \tag{A2}$$

where the positive sign indicates that the outward-flow velocity is increased after the electric field is turned off. Substituting Eqs. (8), (9), and (A2) into Eq. (A1), the following quadratic expression for τ is obtained:

$$\tau^2 - \frac{\eta h}{\gamma}\tau - \frac{\rho h^3}{\gamma} = 0. \tag{A3}$$

The solution of Eq. (A3) gives Eq. (13). Since Eq. (13) is consistent for arbitrary values of the viscosity, Eqs. (10) and (11) are obtained as the approximation of Eq. (13) in the high- and low-viscosity limits, respectively.

[1] D. Mark, S. Haeberle, G. Roth, F. von Stetten, and R. Zengerle, Chem. Soc. Rev. **39**, 1153 (2010).
[2] M. Singh, H. M. Haverinen, P. Dhagat, and G. E. Jabbour, Adv. Mater. **22**, 673 (2010).
[3] L. Pauchard and C. Allain, Phys. Rev. E **68**, 052801 (2003).
[4] L. Pauchard and C. Allain, Europhys. Lett. **62**, 897 (2003).
[5] R. D. Deegan, O. Bakajin, T. F. Dupont, G. Huber, S. R. Nagel, and T. A. Witten, Nature (London) **389**, 827 (1997).
[6] T. Yamada and K. Sakai, Phys. Fluids **24**, 022103 (2012).
[7] J. L. Keddie and A. F. Routh, *Fundamentals of Latex Film Formation* (Springer, Dordrecht, 2010), pp. 95–120.
[8] P. G. de Gennes, Eur. Phys. J. E **7**, 31 (2002).
[9] T. Okuzono, K. Ozawa, and M. Doi, Phys. Rev. Lett. **97**, 136103 (2006).
[10] T. Okuzono and M. Doi, Phys. Rev. E **77**, 030501 (2008).
[11] R. H. Dettre and R. E. Johnson, Jr., J. Colloid Interface Sci. **21**, 367 (1966).
[12] R.-J. Roe, J. Phys. Chem. **72**, 2013 (1968).
[13] K. Sakai and Y. Yamamoto, Appl. Phys. Lett. **89**, 211911 (2006).
[14] E. Raphaël and P. G. de Gennes, Europhys. Lett. **31**, 293 (1995).
[15] E. Raphaël and P. G. de Gennes, Phys. Rev. E **53**, 3448 (1996).
[16] L. D. Landau, E. M. Lifshitz, and L. P. Pitaevskii, *Electrodynamics of Continuous Media*, 2nd ed. (Butterworth-Heinemann, Oxford, 1984), pp. 65–67.
[17] Y. Shimokawa, T. Kajiya, K. Sakai, and M. Doi, Phys. Rev. E **84**, 051803 (2011).
[18] *Handbook of Surface and Colloid Chemistry*, 2nd ed., edited by K. S. Birdi (CRC Press, Boca Raton, FL, 2003), pp. 77–89.
[19] Y. Yoshitake, S. Mitani, K. Sakai, and K. Takagi, J. Appl. Phys. **97**, 024901 (2005).
[20] Datasheet of silicone oils, Shin-Etsu Chemical Co., Ltd.
[21] M. Hosoda, T. Hirano, and K. Sakai, Jpn. J. Appl. Phys. **50**, 07HB03 (2011).